Letter | Editors' Suggestion

Indirect evidence for elemental hydrogen in laser-compressed hydrocarbons

D. Kraus,[1,2] J. Vorberger,[2] N. J. Hartley,[3,2] J. Lütgert,[1,2] M. Rödel,[2,4] D. Chekrygina,[2] T. Döppner,[5] T. van Driel,[3] R. W. Falcone,[6] L. B. Fletcher,[3] S. Frydrych,[5,7] E. Galtier,[3] D. O. Gericke,[8] S. H. Glenzer,[3] E. Granados,[3] Y. Inubushi,[9,10] N. Kamimura,[11] K. Katagiri,[11] M. J. MacDonald,[12,5] A. J. MacKinnon,[3,5] T. Matsuoka,[11] K. Miyanishi,[10] E. E. McBride,[3,13] I. Nam,[3] P. Neumayer,[14] N. Ozaki,[11,15] A. Pak,[5] A. Ravasio,[16] A. M. Saunders,[6] A. K. Schuster,[2,4] M. G. Stevenson,[1] K. Sueda,[10] P. Sun,[3] T. Togashi,[9,10] K. Voigt,[2,4] M. Yabashi,[9,10] and T. Yabuuchi[9,10]

[1]*Institut für Physik, Universität Rostock, Albert-Einstein-Str. 23-24, 18059 Rostock, Germany*
[2]*Helmholtz-Zentrum Dresden-Rossendorf, Bautzner Landstrasse 400, 01328 Dresden, Germany*
[3]*SLAC National Accelerator Laboratory, Menlo Park, California 94025, USA*
[4]*Institute of Solid State and Materials Physics, Technische Universität Dresden, 01069 Dresden, Germany*
[5]*Lawrence Livermore National Laboratory, Livermore, California 94550, USA*
[6]*Department of Physics, University of California, Berkeley, California 94720, USA*
[7]*Institut für Kernphysik, Technische Universität Darmstadt, Schlossgartenstraße 9, 64289 Darmstadt, Germany*
[8]*Centre for Fusion, Space and Astrophysics, Department of Physics, University of Warwick, Coventry CV4 7AL, United Kingdom*
[9]*Japan Synchrotron Radiation Research Institute, 1-1-1 Kouto, Sayo-cho, Sayo-gun, Hyogo 679-5198, Japan*
[10]*RIKEN SPring-8 Center, 1-1-1 Kouto, Sayo-cho, Sayo-gun, Hyogo 679-5148, Japan*
[11]*Graduate School of Engineering, Osaka University, Suita, Osaka 565-0087, Japan*
[12]*Department of Atmospheric, Oceanic, and Space Science, University of Michigan, Ann Arbor, Michigan 48109, USA*
[13]*European XFEL GmbH, Holzkoppel 4, 22869 Schenefeld, Germany*
[14]*GSI Helmholtzzentrum für Schwerionenforschung GmbH, Planckstraße 1, 64291 Darmstadt, Germany*
[15]*Photon Pioneers Center, Osaka University, Suita, Osaka 565-0087, Japan*
[16]*LULI, CNRS, CEA, Sorbonne Université, Ecole Polytechnique - Institut Polytechnique de Paris, 91128 Palaiseau, France*

(Received 25 April 2022; accepted 10 April 2023; published 3 May 2023)

We demonstrate a significantly simplified experimental approach for investigating liquid metallic hydrogen, which is crucial to understand the internal structure and evolution of giant planets. Plastic samples were shock-compressed and then probed by short pulses of X-rays generated by free electron lasers. By comparison with *ab initio* simulations, we provide indirect evidence for the creation of elemental hydrogen in shock-compressed plastics at ∼150 GPa and ∼5, 000 K and thus in a regime where hydrogen is predicted to be metallic. Being the most common form of condensed matter in our solar system, and ostensibly the simplest of all elements, hydrogen is the model case for many theoretical studies and we provide a new possibility to benchmark models for conditions with extreme pressures and temperatures. Moreover, this approach will also allow to probe the chemical behavior of metallic hydrogen in mixture with other elements, which, besides its importance for planetary physics, may open up promising pathways for the synthesis of new materials.

DOI: 10.1103/PhysRevResearch.5.L022023

I. INTRODUCTION

State-of-the-art models of the gas giants Jupiter and Saturn [1,2] predict an interior largely composed of liquid metallic hydrogen. As hydrogen exists in its insulating, molecular form in the outer layers, the insulator-metal transition in liquid hydrogen is crucial for our understanding of these objects as well as many exoplanets.

Creating and investigating liquid metallic hydrogen has been the subject of theoretical and experimental studies for many decades. This state may either be formed by a pressure-induced first-order phase transition, i.e., the "plasma phase transition" [3,4] or a continuous transition at higher temperatures, where the location of the critical point is still under debate [5]. Experimentally, this transformation has mainly been investigated by two distinctly different methods: static compression using diamond anvil cells [6–9] and dynamic compression techniques, e.g., using explosives [10], gas guns [11], pulsed power devices [12], or high-energy lasers [13,14]. Recently, new evidence for the existence for the insulator-metal transition have been achieved by static and dynamic compression methods [7,13]. However, these results are contradictory to previous data [6,12] which may, at least in parts, result from the required experimental complexity.

Experiments compressing hydrogen to metallization conditions are very challenging. Indeed, hydrogen at the high pressures required is difficult to contain in static experiments, whereas dynamic compression experiments usually require

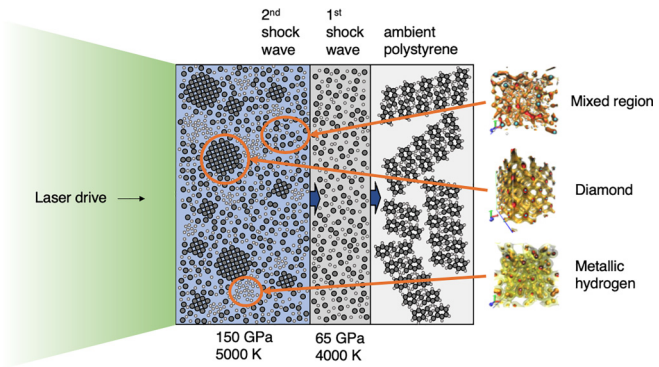

FIG. 1. Schematic concept for creating elemental hydrogen by shock compression of polystyrene. The first shock wave results in dissociation of the polymers while the second shock induces the formation of diamonds and elemental hydrogen. The latter is forming at pressure and temperature conditions where it is predicted to be in a liquid metallic state. The short timescale of the experiment does not allow all carbon and hydrogen to separate and thus there are remaining mixed regions. The different states are illustrated by snapshots from density functional theory and molecular dynamics simulations depicting the atomic positions and isosurfaces of the electron density.

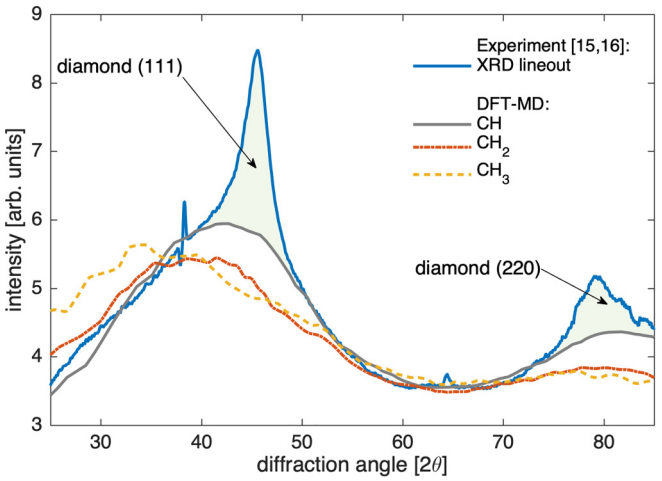

FIG. 2. *In situ* X-ray diffraction (XRD) data at shock coalescence in polystyrene compared to density functional theory and molecular dynamics (DFT-MD) simulations. For the inferred conditions of 150 GPa and 5000 K, the liquid diffraction can only be matched by a C-H ratio of 1:1. From the intensity of the crystalline (111) and (220) diffraction peaks, it can be extracted that ∼50% of all carbon atoms are observed to form a diamond lattice [17]. This also implies that ∼50% of the hydrogen atoms need to cluster in isolated regions that are not mixed with carbon. The photon energy applied for X-ray diffraction was 8.2 keV.

cryogenic liquid hydrogen and large-scale facilities providing sophisticated drive schemes. These complex sample environments severely limit the number of experiments and the diagnostic techniques applicable.

In this Letter, we present a different, less complex method to create metallic hydrogen that utilizes the phase separation, observable as diamond formation, in highly compressed hydrocarbons [15,16]. In double-shocked CH, we observed that about 50% of the carbon atoms inside the sample volume have formed diamond crystal structures at the time when the two shock waves coalesce at the sample rear side, i.e., the time when most of the sample volume is at very similar conditions [17,18]. This observation provides two main options: either the remaining hydrogen is still mixed with the carbon atoms that have not formed diamond or complementary regions of pure hydrogen are forming alongside the diamonds. In the latter case, regions of pure hydrogen will be metallic and regions which are not yet demixed remain in a mixed state with roughly the initial C:H ratio of 1:1. Figure 1 schematically illustrates this scenario that is created by the second shock wave after the first shock has already precompressed and dissociated the polymers of the initial sample material.

II. EXPERIMENTAL RESULTS

We have performed experiments at the Linac coherent light source (LCLS) and at the spring-8 Angstrom compact free electron laser (SACLA) which provide strong evidence for the scenario shown in Fig. 1. Using solid plastic targets, they demonstrate a considerably simplified approach to create metallic hydrogen: at the MEC instrument of LCLS, 83.4 μm thick polystyrene foils were dynamically compressed with high energy lasers launching two subsequent shocks that coalesce after 7.6 ns on the sample rear side. Using *in situ* X-ray diffraction of 8.2 keV photons with ∼0.5% bandwidth and a pulse duration of 50 fs, it was observed that carbon and hydrogen phase separate on nanosecond timescales at pressures of ∼150 GPa and temperatures of ∼5000 K. The observed diffraction features show smooth powder rings where the width and the intensity ratio of the different peaks are compatible with diamond crystallites of few nm in size, which has been discussed in the context of diamond precipitation in the interiors of icy giant planets [15]. More details of the experimental setup have been published in Ref. [16].

Figure 2 shows experimental evidence for regions of elemental hydrogen forming in samples that clearly show diamond formation after shock compression. Here, *in situ* X-ray diffraction (XRD) data from CH samples probed at shock coalescence are compared to predictions from density functional theory combined with molecular dynamics (DFT-MD) simulations of different liquid CH_x mixtures at the pressure and temperature as they were reached in the experiment (see the Supplemental Material for technical details on the simulations [19]). The data shows that the liquid diffraction below the sharp diamond peaks is matched solely by a 1:1 C-H ratio to result in consistent shape and intensity of the two diamond peaks. Any smaller carbon concentration in the mixture would shift the broad liquid correlation peak below the sharper diamond (111) reflection to lower k values, which is not compatible with the measured XRD data. Assuming CH_2 as remaining liquid would produce severely asymmetric peak shapes and the width of the (220) reflection being ∼2x larger than for the (111). At the same time, the relative intensity of the (220) peak would be ∼70% of the (111), where ∼40% would be expected for ambient diamond, which is well matched by assuming CH as the remaining liquid instead. The fact that the number of atoms inside the sample volume

is conserved and the observation that ∼50% of all carbon atoms form diamond implies that there are regions in the compressed samples that are highly enriched with hydrogen. These spatial regions possibly contain pure hydrogen that has fully separated from the carbon in the sample.

A direct signature from hydrogen cannot be recorded due to the very small diffraction strength of the lightest element and the fact that we expect the electrons to be detached from the nuclei. Nonetheless, the existence of elemental hydrogen is further supported by the fact that the diamond growth is an ongoing process after the traversal of the second shock wave. In fact, the observation that ∼50% of carbon atoms have already formed diamond lattices is an average over the entire sample volume. Regions close to the shock front will exhibit a smaller percentage while regions that experienced the second shock earlier have much longer time for diamond formation. These regions will exhibit a much higher diamond fraction and should be close to saturation of this process, which suggests that carbon and hydrogen will fully separate for longer durations of the experiment. Moreover, the 50% estimate does not account for the hotter material in the region with laser-heated plasma, which is too hot to allow stable diamonds and contributes around 10% of the mass in the volume probed with XRD [16]. These facts indicate that demixing of carbon and hydrogen could be complete after conditions for diamond formation have been present in the sample for sufficient time.

We have performed further experiments at the SACLA XFEL that corroborate a complete C-H separation. Polyethylene (CH_2) samples made of 75 μm thick ultra-high-molecular-weight foils of initial density 0.94 g/cm^3 were shockcompressed using the HERMES drive laser system providing energies of 5–22 J in 5 ns flat-top pulses. The drive laser was focused to a spot size of 200 μm resulting in drive intensities of 2.4–10.5 TW/cm^2. An aluminum front layer with a thickness of 100 nm was coated on the sample to prevent low intensity prepulses to preheat the sample. The shock transit time was recorded with a VISAR system showing the impact of the drive laser on the aluminum coating as well as the breakout at the sample rear side. Together with the well-known sample thickness, this provides the shock velocity, which in turn can be used to infer pressure and temperature reached in the sample using first-principles calculations of the polyethylene shock Hugoniot [22]. The microscopic structure was probed *in situ* by the SACLA X-ray pulses with a photon energy of 11.1 keV and ∼0.5% bandwidth. X-ray diffraction patterns were recorded by a flat panel area detector in an angular 2θ-range of 22–77 degrees.

Using these diagnostics, we observe the formation of diamond in a single shock while reaching pressure and temperature regimes comparable to the CH experiment at LCLS (∼150 GPa and ∼4000 K), see Fig. 3. Therefore, mixtures with a CH_2 stoichiometry, which has been seen to resist demixing up to at least 200 GPa at lower temperatures [20,21], are indeed unstable at the conditions of our experiment pointing toward full C-H separation in agreement with the XRD interpretation from double-shocked polystyrene discussed above. A single shock is sufficient to reach carbon-hydrogen phase separation for polyethylene, since the shock Hugoniot curve for this material is predicted to result in significantly

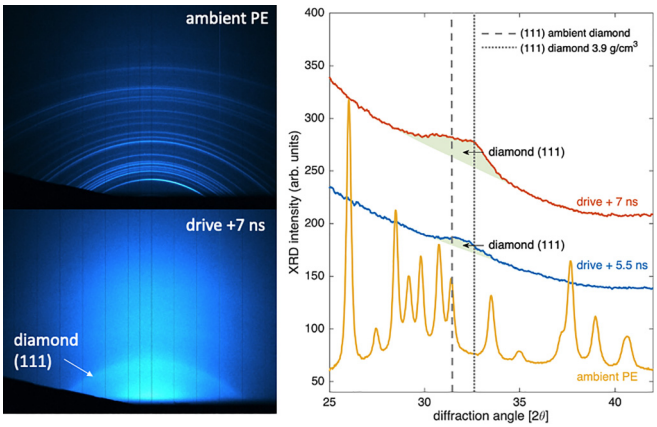

FIG. 3. *In situ* X-ray diffraction data from shock-compressed polyethylene (PE). Left: raw data detector images for ambient conditions and a shock-compressed sample (same color scale). Right: lineouts created by azimuthally integrating the detector images. The lineouts are separated by a constant offset for better feature visibility. Within the shock transit time of ∼5 ns, compressed diamonds are formed. After the shock release, the lattice starts relaxing to ambient density. The photon energy applied for X-ray diffraction was 11.1 keV.

lower temperatures than polystyrene around ∼100 GPa [22]. This specific pressure regime on the CH_2 Hugoniot was not covered in previous *in situ* XRD experiments [23]. Here, diamond formation was not found due to either the lower or higher pressure-temperature conditions investigated. For the SACLA experiments, the relative intensity of the diamond peaks is significantly lower in comparison to the liquid diffraction than observed in the experiments using polystyrene. This fact suggests that the kinetics of diamond formation vary considerably depending on the initial carbon concentration. Nonetheless, the results show that diamond formation is not inhibited as the carbon concentration decreases, although the nucleation rate is reduced.

III. DISCUSSION

Figure 4 illustrates the observed regimes of diamond formation in polyethylene and polystyrene in context with experiments and predictions of the hydrogen insulator-metal transition. Indeed, we only observe rapid diamond formation in a regime where hydrogen is expected to be metallic, similar to the low solubility of carbon in alkali metals at lower temperatures [24]. This indicates that the C-H phase separation reaction may be driven or at least accelerated by hydrogen metallization, similar to the original discussion of H-He demixing inside Saturn and Jupiter [25]. Since we do not directly measure temperature in our experiments, the corresponding values for CH and CH_2 presented in Fig. 4 are obtained from EOS models benchmarked on shock experiments. The error bars shown result from the uncertainties in the measured velocities propagated through the EOS models. In case diamond formation is observed, an additional benchmark for the inferred pressure-temperature conditions is given by the compressed diamond densities extracted from the XRD data [15]. It should be noted that static experiments

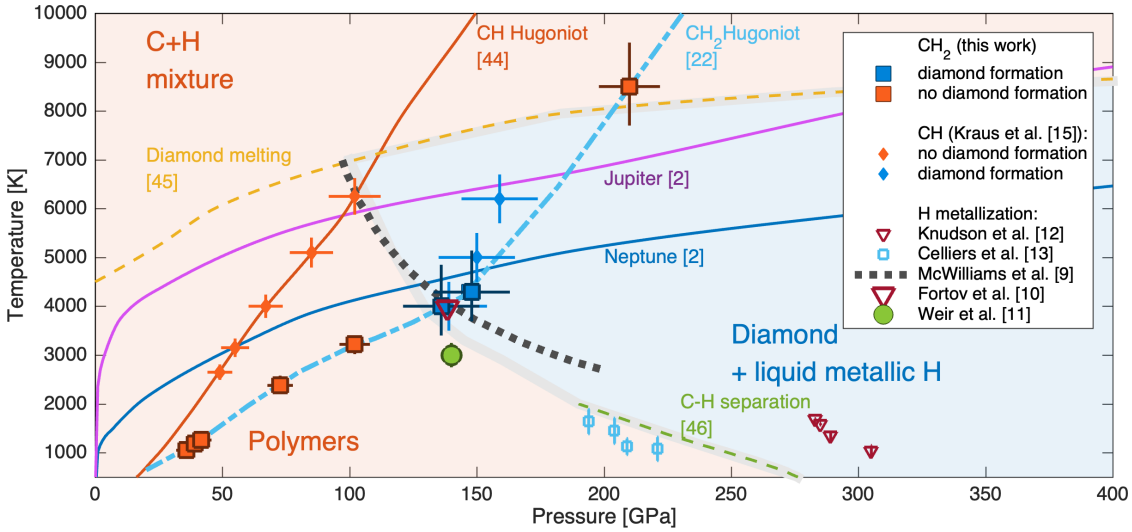

FIG. 4. Pressure-temperature diagram for C-H mixtures under dynamic laser compression on nanosecond timescales. The new CH_2 data is depicted in context with previous CH measurements [15,44] and experiments as well as predictions for the metallization of hydrogen. The regions where we observe the C-H separation coincides reasonably well with the current knowledge of the insulator-metal transition in liquid hydrogen [9–13]. This suggests that below the diamond melting line [45], rapid carbon-hydrogen phase separation may be induced or at least accelerated by hydrogen metallization, which is also compatible with predictions of the C-H separation at lower temperatures [46]. The pressure and temperature values of our CH_2 data are based on first-principles simulations of the polyethylene shock Hugoniot curve [22].

on hydrocarbons employing laser-heated diamond anvil cells suggest a more complex but still inconclusive view at lower pressures around a few 10 GPa. Some studies claim diamond formation in this regime [26,27] while others did not observe diamond structures [28], and the contradictory results may originate from the chemically nonisolated nature of the samples potentially providing catalysis for the C-H separation [15]. Moreover, shock experiments including oxygen in addition to C and H have seen diamond formation at lower *P-T* conditions than pure CH demonstrating the effect of additional elements in the mixture [29,30].

IV. CONCLUSION

A complete C-H separation, even if only accompanied by the formation of liquid metallic hydrogen, enables unprecedented routes to study this important state in dynamic compression experiments. Indeed, experimental setups using plastic foils as initial material are of substantially less complexity compared to the approaches based on cryogenic hydrogen [12–14] or static precompression [31]. Moreover, sample delivery using plastic tapes is compatible with a new generation of dynamic compression experiments with shot rates up to 10 Hz in combination with ultrafast *in situ* X-ray probes, such as provided by the HIBEF infrastructure at the European XFEL [32]. For instance, this will enable experiments using X-ray scattering and spectroscopy methods to measure the bulk conductivity [33] of the compressed samples in contrast to current approaches mostly based on surface reflectivity. Indeed, specifically for the C-H mixture, reflectivity measurements from the shock front in the demixing regime provide an incomplete picture as the phase separation is most likely not completed within an optical skin depth behind the pressure discontinuity [34]. This is supported by the fact that DFT-MD simulations of the C-H mixture at relevant conditions do not show spontaneous demixing for the limited number of a few 100 atoms and timescales of a few ps [16]. By performing bulk measurements with X-rays, uncertainties due to nonequilibrium conditions at the compression fronts or chemical reactions at the window materials can be avoided. Furthermore, by adding other elements into the initial C-H mixture and exploiting precise spectroscopy methods enabled by XFEL facilities [35], it can be studied whether the heteroatoms prefer to react with insulating carbon or metallic hydrogen. This will inform the chemistry and miscibility of planetary interior species, the understanding of which will improve models of the planets in our solar system, including chemistry deep inside our Earth, and the vast and steadily increasing number of known exoplanets. Moreover, specific elements like boron incorporated as dopants into diamonds of only few nanometers in size may have promising applications for imaging and drug delivery in medicine [36], catalysis (e.g., CO_2 reduction reactions [37]), and as quantum sensors [38]. The surface of nanodiamonds may also be functionalized for hydrogen storage to be used in energy applications [39]. This motivates studies of the potential recovery of such doped nanodiamonds formed by lasercompression of doped plastics. Another potential application of the exotic chemistry in this regime is suggested by the fact that recently, hydrogen reacting with heavier elements forming hydride structures at extreme pressures, sometimes including carbon, have increased critical temperatures for superconductivity to the realm of room temperature [40–42]. While those experiments so far have solely been performed with static compression approaches, accessing the kinetics of chemistry at extreme pressure conditions in dynamic experiments will

provide additional model benchmarks for structure searches for this highly interesting class of materials [43].

ACKNOWLEDGMENTS

This work was performed at the Matter at Extreme Conditions (MEC) instrument of LCLS, supported by the U.S. Department of Energy Office of Science, Fusion Energy Science under Contract No. SF00515. D.K., A.M.S., and R.W.F. acknowledge support by the U.S. Department of Energy, Office of Science, Office of Fusion Energy Sciences, Award No. DE-AC02-05CH11231, and National Nuclear Security Administration, Award No. DE-NA0003842. The XFEL experiments on SACLA were performed using BL3 at the EH5 with the approval of the Japan Synchrotron Radiation Research Institute (JASRI) (Proposal No. 2019A8070). D.K., N.J.H., J.L., A.K.S., and K.V. were supported by the Helmholtz Association under VH-NG-1141. SLAC HED is supported by DOE Office of Science, Fusion Energy Science under FWP 100182. S.F. was supported by German Bundesministerium für Bildung und Forschung Project No. 05P15RDFA1. The work of A.P., S.F., and T.D. was performed under the auspices of the U.S. Department of Energy by Lawrence Livermore National Laboratory under Contract No. DE-AC52-07NA27344.

[1] R. Helled, G. Mazzola and R. Redmer, Understanding dense hydrogen at planetary conditions, Nat. Rev. Phys. **2**, 562 (2020).
[2] T. Guillot, Interiors of giant planets inside and outside the solar system, Science **286**, 72 (1999).
[3] G. E. Norman and A. N. Starostin, Thermodynamics of a dense plasma, J. Appl. Spectrosc. **13**, 965 (1970).
[4] W. Ebeling and W. Richert, Plasma phase transition in hydrogen, Phys. Lett. A **108**, 80 (1985).
[5] J. M. McMahon, M. A. Morales, C. Pierleoni and D. M. Ceperley, The properties of hydrogen and helium under extreme conditions, Rev. Mod. Phys. **84**, 1607 (2012).
[6] R. P. Dias and I. F. Silvera, Observation of the Wigner-Huntington transition to metallic hydrogen, Science **355**, 715 (2017).
[7] P. Loubeyre, F. Occelli and P. Dumas, Synchrotron infrared spectroscopic evidence of the probable transition to metal hydrogen, Nature (London) **577**, 631 (2020).
[8] M. I. Eremets and I. A. Troyan, Conductive dense hydrogen, Nat. Mater. **10**, 927 (2011).
[9] R. S. McWilliams, D. A. Dalton, M. F. Mahmood, and A. F. Goncharov, Optical Properties of Fluid Hydrogen at the Transition to a Conducting State, Phys. Rev. Lett. **116**, 255501 (2016).
[10] V. E. Fortov *et al.*, Phase Transition in a Strongly Nonideal Deuterium Plasma Generated by Quasi-Isentropical Compression at Megabar Pressures, Phys. Rev. Lett. **99**, 185001 (2007).
[11] S. T. Weir, A. C. Mitchell, and W. J. Nellis, Metallization of Fluid Molecular Hydrogen at 140 GPa (1.4 Mbar), Phys. Rev. Lett. **76**, 1860 (1996).
[12] M. D. Knudson, M. P. Desjarlais, A. Becker, R. W. Lemke, K. R. Cochrane, M. E. Savage, D. E. Bliss, T. R. Mattsson and R. Redmer, Direct observation of an abrupt insulator-to-metal transition in dense liquid deuterium, Science **348**, 1455 (2015).
[13] P. M. Celliers *et al.*, Insulator-metal transition in dense fluid deuterium, Science **361**, 677 (2018).
[14] P. Davis *et al.*, X-ray scattering measurements of dissociation-induced metallization of dynamically compressed deuterium, Nat. Commun. **7**, 11189 (2016).
[15] D. Kraus *et al.*, Formation of diamonds in laser-compressed hydrocarbons at planetary interior conditions, Nature Astronomy **1**, 606 (2017).
[16] D. Kraus *et al.*, High-pressure chemistry of hydrocarbons relevant to planetary interiors and inertial confinement fusion, Phys. Plasmas **25**, 056313 (2018).
[17] A.K. Schuster, N.J. Hartley, J. Vorberger, T. Doppner, T. vanDriel, R.W. Falcone, L.B. Fletcher, S. Frydrych, E. Galtier, E.J. Gamboa, D.O. Gericke, S.H. Glenzer, E. Granados, M.J. MacDonald, A.J. MacKinnon, E.E. McBride, I. Nam, P. Neumayer, A. Pak, I. Prencipe, K. Voigt, A.M. Saunders, P. Sun, and D. Kraus, Measurement of diamond nucleation rates from hydrocarbons at conditions comparable to the interiors of icy giant planets, Phys. Rev. B **101**, 054301 (2020).
[18] S. Frydrych *et al.*, Demonstration of X-ray Thomson scattering as diagnostics for miscibility in warm dense matter, Nat. Commun. **11**, 2620 (2020).
[19] See Supplemental Material at http://link.aps.org/supplemental/10.1103/PhysRevResearch.5.L022023 for CH_2 XRD raw data and details of the ab initio calculations done with DFT-MD.
[20] N. J. Hartley *et al.*, Evidence for crystalline structure in dynamically-compressed polyethylene up to 200 GPa, Sci. Rep. **9**, 4196 (2019).
[21] L. J. Conway and A. Hermann, High pressure hydrocarbons revisited: From van der waals compounds to diamond, Geosciences **9**, 227 (2019).
[22] T. R. Mattsson, J. M. D. Lane, K. R. Cochrane, M. P. Desjarlais, A. P. Thompson, F. Pierce and G. S. Grest, First-principles and classical molecular dynamics simulation of shocked polymers, Phys. Rev. B **81**, 054103 (2010).
[23] N.J. Hartley, J. Vorberger, T. Doppner, T. Cowan, R.W. Falcone, L.B. Fletcher, S. Frydrych, E. Galtier, E.J. Gamboa, D.O. Gericke, S.H. Glenzer, E. Granados, M.J. MacDonald, A.J. MacKinnon, E.E. McBride, I. Nam, P. Neumayer, A. Pak, K. Rohatsch, A.M. Saunders, A.K. Schuster, P. Sun, T. vanDriel, and D. Kraus, Liquid Structure of Shock-Compressed Hydrocarbons at Megabar Pressures, Phys. Rev. Lett. **121**, 245501 (2018).
[24] B. Longson and A. W. Thorley, Solubility of carbon in sodium, J. Appl. Chem. **20**, 372 (1970).
[25] D. J. Stevenson and E. E. Salpeter, The phase diagram and transport properties for hydrogen-helium fluid planets, Astrophys. J. Suppl. Series **35**, 221 (1977).
[26] L. R. Benedetti *et al.*, Dissociation of CH4 at high pressures and temperatures: diamond formation in giant planet interiors? Science **286**, 100 (1999).
[27] H. Hirai, K. Konagai, T. Kawamura, Y. Yamamoto, and T. Yagi, Polymerization and diamond formation from melting methane and their implications in ice layer of giant planets, Phys. Earth Planet. Inter. **174**, 242 (2009).
[28] S. S. Lobanov *et al.*, Carbon precipitation from heavy hydro-

carbon fluid in deep planetary interiors, Nat. Commun. **4**, 2446 (2013).

[29] M. C. Marshall *et al.*, Diamond formation in double-shocked epoxy to 150 GPa, J. Appl. Phys. **131**, 085904 (2022).

[30] Z. He *et al.*, Diamond formation kinetics in shock-compressed C-H-O samples recorded by small-angle x-ray scattering and x-ray diffraction, Sci. Adv. **8**, eabo0617 (2022).

[31] S. Brygoo *et al.*, Evidence of hydrogen-helium immiscibility at Jupiter-interior conditions, Nature (London) **593**, 517 (2021).

[32] U. Zastrau *et al.*, Conceptual Design Report: Dynamic Laser Compression Experiments at the HED Instrument of European XFEL, European XFEL Report 2017-004 (2017), doi:10.22003/XFEL.EU-TR-2017-001.

[33] B. B. L. Witte, L. B. Fletcher, E. Galtier, E. Gamboa, H. J. Lee, U. Zastrau, R. Redmer, S. H. Glenzer and P. Sperling, Warm Dense Matter Demonstrating Non-Drude Conductivity from Observations of Nonlinear Plasmon Damping, Phys. Rev. Lett. **118**, 225001 (2017).

[34] N. J. Hartley *et al.*, Dynamically pre-compressed hydrocarbons studied by self-impedance mismatch, Matter Radiat. Extremes **5**, 028401 (2020).

[35] K. Voigt *et al.*, Demonstration of an x-ray Raman spectroscopy setup to study warm dense carbon at the high energy density instrument of European XFEL, Phys. Plasmas **28**, 082701 (2021).

[36] G. Hong, S. Diao, A. L. Antaris and H. Dai, Carbon nanomaterials for biological imaging and nanomedicinal therapy, Chem. Rev. **115**, 10816 (2015).

[37] Y. Liu *et al.*, Selective Electrochemical Reduction of Carbon Dioxide to Ethanol on a Boron- and Nitrogen-Co-doped Nanodiamond, Angew. Chem. **129**, 15813 (2017).

[38] J. R. Maze *et al.*, Nanoscale magnetic sensing with an individual electronic spin in diamond, Nature (London) **455**, 644 (2008).

[39] L. Lai and A. S. Barnard, Nanodiamond for hydrogen storage: Temperature-dependent hydrogenation and charge-induced dehydrogenation, Nanoscale **4**, 1130 (2012).

[40] E. Snider, N. Dasenbrock-Gammon, R. McBride, M. Debessai, H. Vindana, K. Vencatasamy, K. V. Lawler, A. Salamat ans R. P. Dias, Room-temperature superconductivity in a carbonaceous sulfur hydride, Nature (London) **586**, 373 (2020).

[41] A. P. Drozdov, M. I. Eremets, I. A. Troyan, V. Ksenofontov and S. I. Shylin, Conventional superconductivity at 203 kelvin at high pressures in the sulfur hydride system, Nature (London) **525**, 73 (2015).

[42] A. P. Drozdov *et al.*, Superconductivity at 250 K in lanthanum hydride under high pressures, Nature (London) **569**, 528 (2019).

[43] C. J. Pickard, I. Errea and M. I. Eremets, Superconducting hydrides under pressure, Annu. Rev. Condens. Matter Phys. **11**, 57 (2020).

[44] M. A. Barrios, D. G. Hicks, T. R. Boehly, D. E. Fratanduono, J. H. Eggert, P. M. Celliers, G. W. Collins and D. D. Meyerhofer, High-precision measurements of the equation of state of hydrocarbons at 1-10 Mbar using laser-driven shock waves, Phys. Plasmas **17**, 056307 (2010).

[45] X. Wang, S. Scandolo and R. Car, Carbon Phase Diagram from *Ab Initio* Molecular Dynamics, Phys. Rev. Lett. **95**, 185701 (2005).

[46] G. Gao, A. R. Oganov, Y. Ma, H. Wang, P. Li, Y. Li, T. Iitaka and G. Zou, Dissociation of methane under high pressure, J. Chem. Phys. **133**, 144508 (2010).